Inhibition of NF-κB activation in macrophages increases atherosclerosis in LDL receptor–deficient mice

Edwin Kanters,[1] Manolis Pasparakis,[2] Marion J.J. Gijbels,[3,4] Monique N. Vergouwe,[3] Iris Partouns-Hendriks,[3] Remond J.A. Fijneman,[1] Björn E. Clausen,[5] Irmgard Förster,[6] Mark M. Kockx,[7] Klaus Rajewsky,[8] Georg Kraal,[1] Marten H. Hofker,[3] and Menno P.J. de Winther[3]

[1]Department of Molecular Cell Biology and Immunology, Vrije Universiteit Medical Center, Amsterdam, The Netherlands
[2]European Molecular Biology Laboratory, Mouse Biology Programme, Monterotondo, Italy
[3]Department of Molecular Genetics, and
[4]Department of Pathology, Cardiovascular Research Institute Maastricht, Maastricht University, Maastricht, The Netherlands
[5]Department of Cell Biology and Histology, Academic Medical Center, Amsterdam, The Netherlands
[6]Institute for Medical Microbiology, Immunology and Hygiene, Technical University of Munich, Munich, Germany
[7]Department of Pathology, Middelheim General Hospital, Antwerp, Belgium
[8]Center for Blood Research, Harvard Medical School, Boston, Massachusetts, USA

Atherosclerosis is now generally accepted as a chronic inflammatory condition. The transcription factor NF-κB is a key regulator of inflammation, immune responses, cell survival, and cell proliferation. To investigate the role of NF-κB activation in macrophages during atherogenesis, we used LDL receptor–deficient mice with a macrophage-restricted deletion of IκB kinase 2 (IKK2), which is essential for NF-κB activation by proinflammatory signals. These mice showed increased atherosclerosis as quantified by lesion area measurements. In addition, the lesions were more advanced and showed more necrosis and increased cell number in early lesions. Southern blotting revealed that deletion of IKK2 was approximately 65% in macrophages, coinciding with a reduction of 50% in NF-κB activation, as compared with controls. In both groups, the expression of differentiation markers, uptake of bacteria, and endocytosis of modified LDL was similar. Upon stimulation with LPS, production of TNF was reduced by approximately 50% in IKK2-deleted macrophages. Interestingly, we also found a major reduction in the anti-inflammatory cytokine IL-10. Our data show that inhibition of the NF-κB pathway in macrophages leads to more severe atherosclerosis in mice, possibly by affecting the pro- and anti-inflammatory balance that controls the development of atherosclerosis.

J. Clin. Invest. **112**:1176–1185 (2003). doi:10.1172/JCI200318580.

Introduction

Atherosclerosis is regarded as a chronic inflammatory disease of the vessel wall, characterized by the accumulation of lipid-laden macrophages and fibrous material in the large arteries (1, 2). An initiating event is the accumulation of lipids, mainly LDLs in the vessel wall, which subsequently will become modified and trigger an inflammatory process. Monocytes are then attracted from the blood and differentiate into macrophages that take up the modified LDL and will form lipid-laden foam cells, which is the first hallmark of atherosclerotic plaque development. Later on, inflammatory mediators will increase, other immune cells will be attracted, and smooth muscle cells will be activated and become involved. More advanced stages of plaque development are characterized by increased deposition of extracellular lipid cores, fibrous material, and often necrosis. Subsequently, these macrophages are further activated, leading to the production of a wide range of cytokines and growth factors (3). Hence, atherogenesis is an inflammatory process in which the macrophage is the major player.

The transcription factor NF-κB is one of the key regulators of inflammation, immune responses, and cell survival. Upon activation, NF-κB can mediate the induction of more than 160 genes, many of which have a documented role in atherogenesis (4). Activated NF-κB has been detected in endothelial cells, smooth muscle cells, and macrophages in atherosclerotic plaques (5).

NF-κB is a family of transcription factors consisting of five members: p65 (relA), c-Rel, relB, p50, and p52. These proteins form homo- or heterodimers of which p65p50 is the most abundant. In resting cells, NF-κB dimers are kept inactive associated with inhibitory

Received for publication April 8, 2003, and accepted in revised form August 13, 2003.

Address correspondence to: Menno P.J. de Winther, Department of Molecular Genetics, Cardiovascular Research Institute Maastricht UNS50/11, Universiteitssingel 50, 6229ER Maastricht, The Netherlands. Phone: 31-43-3881897; Fax: 31-43-3884574; E-mail: dewinther@gen.unimaas.nl.
Edwin Kanters and Manolis Pasparakis contributed equally to this work.

Conflict of interest: The authors have declared that no conflict of interest exists.

Nonstandard abbreviations used: IκB kinase (IKK); LDL receptor knockout (*Ldlr*$^{-/-}$); NF-κB essential modulator (NEMO); bone marrow–derived macrophages (BMM); relative electrophoretic mobility (rem).

proteins, the IκBs. NF-κB activation is mediated by the IκB kinase (IKK) complex containing two catalytic subunits, IKK1 (IKKα) and IKK2 (IKKβ), and a regulatory subunit called NF-κB essential modulator (NEMO or IKKγ). Upon stimulation, the IKK complex phosphorylates IκB, inducing its ubiquination and subsequent degradation. NF-κB is then free to the translocate to the nucleus where it facilitates the transcription of many genes, including proinflammatory cytokines, chemokines, and antiapoptotic factors (6). IKK2 plays a critical role in the activation of NF-κB by proinflammatory signals, as shown by severely impaired NF-κB activation of IKK2-deficient fibroblasts in response to IL-1 or TNF (7, 8). IKK2-deficient mice die from massive TNF-dependent liver apoptosis at embryonic days 12.5–14.5, similarly to mice lacking NEMO or p65.

Here we use macrophage-restricted deletion of IKK2 to investigate the role of NF-κB activation in macrophages in the development of atherosclerosis. To establish such a model, mice carrying an IKK2 allele flanked by loxP sites (floxed) (9) were crossed to LysMCre mice (10), expressing Cre-recombinase in macrophages and granulocytes. The resulting mice carried homozygous floxed IKK2 alleles and were either WT ($IKK2^{fl}$) or heterozygous knock-in for LysMCre ($IKK2^{del}$).

Methods

Mice and diet. Mice carrying the floxed IKK2 gene (9) were crossed to LysMCre mice (10) to obtain mice with a homozygously floxed IKK2 gene and either WT or heterozygous knock-in for LysMCre ($IKK2^{fl}$ and $IKK2^{del}$, respectively). The $IKK2^{fl}$ and $IKK2^{del}$ mice used in these experiments were backcrossed to C57Bl6 five times. LDL receptor–knockout ($Ldlr^{-/-}$) mice were described elsewhere (11) and had been crossed back to C57Bl6 four times. A high-fat diet (Hope Farms, Woerden, The Netherlands) contained 16% fat, 0.15% cholesterol, and no cholate. All experiments were approved by the Committee for Animal Welfare of Maastricht University.

Bone marrow transplantation. One week before transplantation, $Ldlr^{-/-}$ mice were put in filter-top cages and on acidified water containing neomycin (100 mg/l) and polymyxin B sulphate (60,000 U/l). One day prior to transplantation, the mice were subjected to total body irradiation (10 Gy, roentgen source). For transplantation, mice (20 and 18 recipient $Ldlr^{-/-}$ mice, for $IKK2^{fl}$ and $IKK2^{del}$, respectively) were injected intravenously with 10^7 bone marrow cells from pools of bone marrow from either five $IKK2^{fl}$ mice or five $IKK2^{del}$ mice (all littermates).

Blood analysis. Four weeks after transplantation, the mice were fed a high-fat diet for 10 weeks. After 8 weeks of the diet, blood was drawn after overnight fast for lipid and leukocyte analysis and chimerism determination. Plasma cholesterol and triglyceride levels were determined using enzymatic kits (Sigma-Aldrich, Zwijndrecht, The Netherlands, catalog nos. 401 and 337). Lipoprotein profiles were determined on pooled plasma samples using an AKTABasic chromotography system with a Superose 6PC 3.2/30 column (Amersham Biosciences, Roosendaal, The Netherlands). For leukocyte analysis, 25 μl blood was washed extensively in erythrocyte lysis buffer (0.155 M NH_4CL, 10 mM $NaHCO_3$). Cells were stained either with Mac1-PE and Gr1-FITC or with 6B2-PE and KT3-FITC (BD Sciences Pharmingen, San Diego, California, USA) in PBS containing 5% normal mouse serum and 1% FCS. After 1 hour, cells were washed and analyzed by FACS analysis (Facssort, BD Sciences Pharmingen). Leukocytes were discriminated by the following criteria: T cells were KT3 positive, B cells 6B2 positive, monocytes Mac1 positive/Gr1 negative, and granulocytes Gr1 positive.

Atherosclerosis. At 10 weeks, mice were killed, and the heart was isolated as described (12). Sections (7 μm) were cut out of the heart in the area where the atrioventricular valves were visible. Sections were routinely stained with toluidin for morphometric analysis and characterization of the lesions and with Sirius red for collagen. In addition, sections were stained with antibodies against T cells (CD4 and CD8) and macrophages (MOMA-2), as described previously (13). TUNEL-positive cells were stained as described before (14). For lesion area measurements, six toluidin-stained sections, with an interval of 42 μm, were analyzed. All additional analysis was done using randomly selected single sections from within the same area as that was used for lesion area measurements. Scion Image software (Scion Corp., Frederick, Maryland, USA) was used for lesion area, necrotic area, and Sirius red quantification. All analyses were performed without prior knowledge of the genotype.

Determination of chimerism and deletion by Taqman. To determine the chimerism in transplanted mice, we took advantage of the fact that the donor bone marrow was $Ldlr^{WT}$, whereas recipient bone marrow was $Ldlr^{-/-}$. Genomic DNA was isolated using the GFX Genomic DNA Purification Kit (Amersham Pharmacia Biotech Inc., Arlington Heights, Illinois, USA). A standard curve was generated using DNA from $Ldlr^{-/-}$ and $Ldlr^{WT}$ bone marrow cells, mixed at different ratios. Chimerism was determined by quantifying the amount of $Ldlr^{-/-}$ DNA in samples from 40 μl peripheral blood. To standardize for the amount of input DNA, a nonrelevant gene was quantified (p50). Samples were assayed in duplicate using the TaqMan Universal PCR Master Mix (UMM) and the 7700 Sequence Detector (Applied Biosystems, Foster City, California, USA) using 300 nM primer and 200 nM probe. The $Ldlr^{-/-}$ specific primer/probe set was: forward 5′-GCTGCAACTCATCCATATGCA-3′; reverse 5′-GGAGTTGTTGACCTCGACTCTAGAG-3′; probe 5′-6FAM-CCCCAGTCTTTGGGCCTGCGA-TAMRA-3′. The p50-specific primer/probe set was: forward 5′-AACCTG-GGAATACTTCATGTGACTAA-3′; reverse 5′-GCACCAGA-AGTCCAGGATTATAGC-3′; probe 5′-TET-TCCGTGCTT-CCAGTGTTTCAAATACCTTTTT-TAMRA-3′. The data were analyzed using the Sequence Detection Software

(Applied Biosystems). A standard curve was generated by plotting the mean Δ Ct ($Ct_{p50} - Ct_{Ldlr^{-/-}}$) against the logarithm of the percentage $Ldlr^{-/-}$ and calculation of a regression line. Chimerism was calculated from the percentage of $Ldlr^{-/-}$ DNA in the blood samples (representing the remaining recipient bone marrow), determined by applying the mean delta Ct of the sample to the standard curve. Deletion of IKK2 in FACS populations was determined by a similar approach. The standard curve was composed of genomic DNA of WT and $IKK2^{fl}$ bone marrow cells mixed at different ratios. The percentage of deletion can be derived from the quantified amount of $IKK2^{fl}$ allele. Primer/probe set for these assays was: forward 5′-AGTCGAGGCCGCTCTAGAACT-3′; reverse 5′-TCTTGACACATTTTCTGACTTTTGAGT-3′; probe 5′-FAM-TGGATCCCCCGGGCTGCA-TAMRA-3′. To standardize for the amount of input DNA, again a nonrelevant gene was quantified (p50).

Quantification of deletion of IKK2 by Southern blotting. Southern blotting for quantification of the deletion was essentially performed as described before (9). Briefly, DNA was isolated from cells and digested with StuI. Southern blots were made and hybridized with a 700-bp probe, detecting a 3.8-kb WT allele, a 3.9-kb floxed allele, or a 1.8-kb deleted allele. Blots were exposed and bands were quantified using a Bio-Rad Personal Molecular Imager FX System and Quantity One software (Bio-Rad Laboratories Inc., Hercules, California, USA). Ratios between the different bands were used to quantify deletion efficiency.

Bone marrow–derived macrophages. Bone marrow–derived macrophages (BMM) were obtained according to standard procedures described elsewhere (15). All cultures and analyses of BMM were performed in R10 (RPMI1640-10% FCS, 100 U/ml penicillin, 100 μg/ml streptomycin, 2 mM L-glutamine, and 10 mM Hepes) with the addition of 15% L929-cell–conditioned medium (LCM) (16), except stated otherwise. After seeding, the cells were left to adhere for 20 hours before experiments were performed.

NF-κB activation assay. BMM were seeded on bacteriologic plastic six-well plates (Greiner, Alphen aan den Rijn, The Netherlands) at 2×10^6 cells per well. Cells were stimulated with 10 ng/ml LPS for 0, 10, and 60 minutes, respectively. Next, nuclear extracts were isolated as described (17). p65 activation was quantified using an oligonucleotide-based ELISA (Active Motif, Rixensart, Belgium) according to the supplier's instructions. The background was assessed by incubation with binding buffer only. Controls included stimulated Hela cells, competition with free NF-κB oligo, and competition with free mutated NF-κB oligo.

Surface markers and uptake of Escherichia coli and modified LDL. BMM were stained for eight macrophage differentiation markers according to standard procedures. Antibodies used were MAC1 (CD11b/CD18), MAC2 (galectin 3), MAC3, SER4 (sialoadhesion), FA11 (macrosialin), F4/80, M5/114 (MHC class xII), and ED31 (MARCO). Control consisted of the ablation of the primary antibody. Both bacterial uptake and uptake of modified LDL was performed in Optimem-1 for 3 hours using BMM seeded on bacteriologic plastic 24-well plates (Greiner) at 5×10^5 cells per well. *E. coli* (DH5α) containing an expression vector with Green Fluorescent Protein under the control of the LacZ promoter (a generous gift of Guillaume van Eys, Maastricht University) was used at indicated doses. Uptake was blocked by 30 min. preincubation and coincubation with 2 μM cytochalasin D. Acetylated LDL and oxidized LDL were generated and labeled with the fluorescent lipid 1,1′-dioctadecyl-3,3,3′,3′-tetramethylindocarbocyanine perchlorate (DiI) (Molecular Probes, Leiden, The Netherlands) as described (18). The modifications of LDL were checked by assaying the relative electrophoretic mobility (rem) on agarose gel (19). The rem for LDL was set to 1. Acetylated LDL had a rem of 3.8, whereas the rem of oxidized LDL was 3.1. For determination of cell death, cells were plated in 24-well plates at 5×10^5 cells per well and incubated with the indicated concentration of LPS and/or oxLDL. Next, cells were lifted, washed in ice-cold PBS, and incubated with propidium iodide (10 μg/ml) for 30 minutes. All assays were analyzed by FACS analysis (FACSort, BD Biosciences, San Jose, California, USA).

Intracellular TNF staining and cytokine secretion. Macrophages were seeded on bacteriologic plastic 24-well plates at 5×10^5 cells per well. TNF production was quantified in response to 3 hours treatment with LPS (O111:B4, Sigma-Aldrich) by intracellular cytokine staining, as described before (20). For separation of TNF^- and TNF^+ populations and subsequent deletion quantification, cells were activated, stained similarly, and purified on a MoFlo sorter (DakoCytomation, Carpinteria, California, USA). For cytokine secretion, cells were stimulated with 10 ng/ml LPS for the indicated times and cytokine levels of IL-6, IL-10, IL-12 were assayed in the supernatants by ELISA (Biosource, Etten-leur, The Netherlands). For some experiments, recombinant IL-10 (Immunosource, Halle-Zoersel, Belgium) was added at the indicated concentrations at the same time as LPS. Blocking of IL-10 secretion was performed using purified rat-anti-mouse IL-10 (clone 2A5) or IgG control at a concentration of 20 μg/ml, added at the same time as LPS.

Isolation of resident and thioglycollate-elicited peritoneal macrophages. For determination of deletion, resident peritoneal macrophages were isolated from three to five mice per group and purified by FACS ($CD11b^{high}/CD19^-$). For isolation of elicited peritoneal macrophages, mice were injected intraperitoneally with 1 ml of sterile thioglycollate broth (4% wt/vol). After 4 days, cells were isolated by flushing the peritoneum with 8 ml ice-cold PBS. Red blood cells were lysed and the remaining cells were extensively washed using ice-cold PBS. Cells were seeded on bacteriologic plastic. After 2 hours, plates were washed and adherent cells were lifted, using 4 mg/ml lidocaine dissolved

Table 1
Chimerism, relative blood leukocytes, and lipid levels of *Ldlr*$^{-/-}$ mice transplanted with donor bone marrow of indicated genotype

	IKK2^{fl}	IKK2^{del}
White blood cells of donor origin (%)	95.6 ± 2.1	95.3 ± 2.5
T cells (%)	32.0 ± 5.1	33.2 ± 5.3
B cells (%)	42.5 ± 6.7	43.7 ± 5.3
Granulocytes (%)	6.7 ± 2.9	5.7 ± 1.6
Monocytes (%)	6.2 ± 1.5	6.2 ± 0.8
Plasma cholesterol (mM)	19.5 ± 4.4	21.9 ± 4.8
Plasma triglycerides (mM)	1.4 ± 0.6	1.2 ± 0.6

in PBS-10 mM EDTA and counted. Cells were used for DNA isolation or intracellular TNF staining. Macrophages were identified as F4/80^{+} cells.

Statistical analysis. All statistical analyses were performed using GraphPad Prism (GraphPad Software Inc., San Diego, California, USA). Data were analyzed for normality using the Kolmogorov-Smirnov test. All data followed normal distribution and were tested using Welch's corrected *t* test, unless otherwise stated. $P < 0.05$ was considered significant.

Results

Deletion of IKK2 in macrophages does not affect chimerism after bone marrow transplantation, relative numbers of blood leukocytes, or lipid parameters. Bone marrow from IKK2^{fl} or IKK2^{del} mice was transplanted to 10-week-old, lethally irradiated LDL receptor-deficient mice (*Ldlr*$^{-/-}$) to yield chimeric *Ldlr*$^{-/-}$ mice with either IKK2^{fl} macrophages (IKK2^{fl} → *Ldlr*$^{-/-}$) or IKK2^{del} macrophages (IKK2^{del} → *Ldlr*$^{-/-}$). After 4 weeks recovery, the mice were fed a high-fat diet for 10 weeks. At 8 weeks of diet, we collected blood and determined chimerism in white blood cells using quantitative real-time PCR. On average 95% of the white blood cells were of donor origin, confirming successful engraftment. Chimerism was equal in the IKK2^{fl}- and IKK2^{del}-transplanted groups (Table 1). Relative levels of T cells, B cells, monocytes, and granulocytes were normal and were not different between groups (Table 1). In addition, plasma cholesterol and triglyceride levels were similar (Table 1). Lipoprotein profile analysis revealed no differences between the two groups (Figure 1).

Deletion of IKK2 in macrophages increases atherosclerosis in Ldlr$^{-/-}$ *mice*. We killed the mice after 10 weeks of a high-fat diet and analyzed atherosclerosis in the aortic root. Lesions were mainly composed of macrophages with some fibrotic cap formation (Figure 2a and b). Lesion area measurements revealed a striking 62% increase in the IKK2^{del}-transplanted mice, as compared with controls (Figure 2c). Thus, inhibition of NF-κB activation in macrophages resulted in an increase in atherosclerotic lesion formation.

Increased necrosis in lesions of Ldlr$^{-/-}$ *mice transplanted with IKK2*^{del}. During pathological examination of the lesions, we scored necrosis by the presence of pyknosis, karyorrhexis, or complete absence of nuclei. Surprisingly, the IKK2^{del}-transplanted group had many more lesions that showed characteristics of necrosis (Figure 3a and b). Some 50% of the IKK2^{del}-transplanted mice had atherosclerotic lesions with necrosis as compared with only 5% of the IKK2^{fl}-transplanted mice (Figure 3c). Quantification of necrotic area size revealed that IKK2^{fl}-transplanted mice had 1.2% ± 1.2% necrosis in their plaques, whereas IKK2^{del}-transplanted animals had 6.1% ± 2.1% necrosis ($P < 0.05$, Mann Whitney *U* test). Since NF-κB has been shown to be involved in apoptosis (7, 8, 21, 22), and our necrosis quantification could not distinguish between necrosis and apoptosis, we examined the presence of apoptotic cells in the lesions by TUNEL staining. Levels of TUNEL-positive cells were equal between control and IKK2^{del}-transplanted mice (Figure 3d), indicating no difference in levels of apoptosis.

Two additional characteristics of plaque progression were quantified: influx of T cells and formation of a fibrous cap. We quantified T cells by staining for CD4 and CD8. Both the cumulative number (Figure 3e) and the separate number (not shown) of CD4- and CD8-positive cells were equal between the groups. To quantify fibrosis, we stained collagen in lesions using Sirius red and quantified the area in positive lesions. No differences were observed between the IKK2^{fl} and IKK2^{del} groups (Figure 3f).

More advanced plaques and increased cell number in early lesions of Ldlr$^{-/-}$ *mice transplanted with IKK2*^{del}. To further explore the characteristics of atherosclerosis, we categorized the lesions essentially as described previously (23). Three types of lesions were discerned: (1) early lesions were fatty streaks containing only foam cells (2) moderate lesions were characterized by the additional presence of a collagenous cap, and (3) advanced lesions showed involvement of the media and increased collagen content. The amount of each type as a percentage of all the lesions is expressed in Figure 4a. It is clear that there is a shift towards more severe

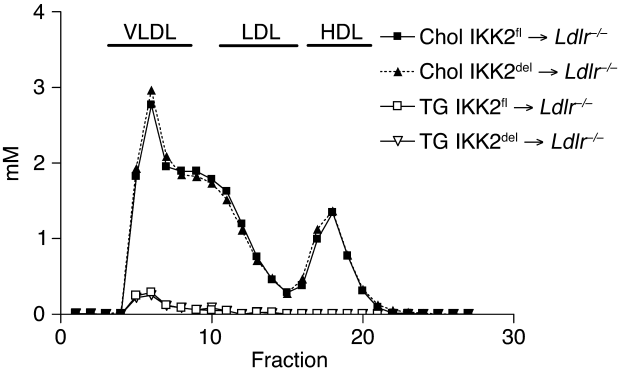

Figure 1
Plasma lipoprotein profiles of IKK2^{fl}- and IKK2^{del}-transplanted *Ldlr*$^{-/-}$ mice after 8 weeks of high-fat feeding. Indicated are cholesterol levels (Chol) and triglyceride levels (TG) after size fractionation of pooled plasma samples.

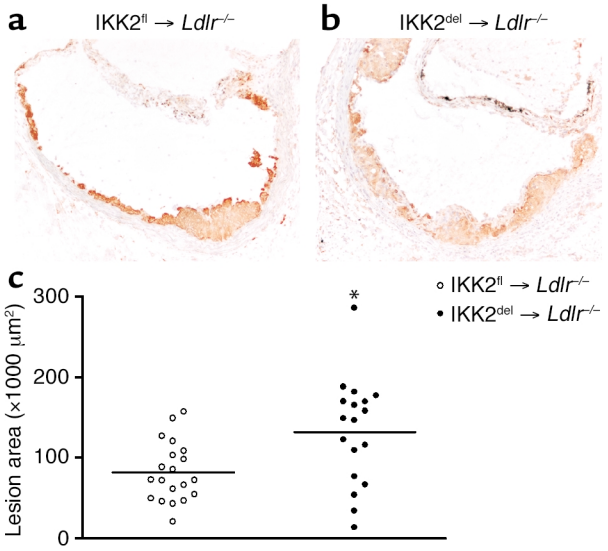

Figure 2
Atherosclerosis in IKK2^{fl}- and IKK2^{del}-transplanted *Ldlr*$^{-/-}$ mice. (**a**) Representative lesions from *Ldlr*$^{-/-}$ mice transplanted with IKK2^{fl} and (**b**) IKK2^{del} BMM using MOMA-2. (**c**) Atherosclerotic lesion area in IKK2^{fl}-transplanted (open circles, $n = 20$) and IKK2^{del}-transplanted (closed circles, $n = 18$) *Ldlr*$^{-/-}$ mice. Circles indicate individual mice. *$P < 0.01$.

lesions in the IKK2^{del} group, indicating enhanced progression of atherosclerosis. To investigate whether NF-κB is also involved in the early steps of atherogenesis, we analyzed the size of the early lesions. Indeed, early lesions were significantly larger in the IKK2^{del} group (Figure 4b). Cell counting revealed that this was attributable to an increase in the number of cells in the lesions (Figure 4c) and not to an increase in size of the foam cells (Figure 4d). These data show that atherosclerosis in the IKK2^{del} group is characterized by an increase of inflammatory cells early on in the development of the lesions and by an increase in the rate of progression of atherogenesis.

NF-κB activation is severely impaired in BMM from IKK2^{del} mice. To study the in vitro phenotype of IKK2^{del} macrophages, we cultured BMM from IKK2^{fl} and IKK2^{del} mice. The yields of macrophages from both mice were the same (not shown). The degree of inhibition of NF-κB in IKK2^{del} macrophages is dependent on the effectiveness of Cre-recombinase in deleting the loxP-flanked IKK2 gene. To examine the deletion efficiency in IKK2^{del} macrophages, we performed Southern blotting (Figure 5a). Quantitative analysis revealed that in different cultures the deletion was approximately 60%–70%. To quantify the effect of deletion on NF-κB activation, we used an ELISA-based assay, examining DNA binding of p65 in nuclear extracts. IKK2^{del} macrophages showed approximately 40%–50% less p65 activation at 10 and 60 minutes, respectively, after stimulation with LPS (Figure 5b). These data show that although deletion of the IKK2 gene was not complete, NF-κB activation is severely impaired in IKK2^{del} macrophages.

Deletion of IKK2 in BMM does not affect differentiation, bacterial uptake, and endocytosis of modified LDL. To investigate whether inhibition of NF-κB affects macrophage differentiation, the expression of six macrophage-specific differentiation markers was examined by FACS analysis. No differences were found between IKK2^{fl} and IKK2^{del} macrophages (Figure 5c). In addition, no expression of MHC-classII and MARCO was found, which are specific markers for activated macrophages and marginal zone macrophages, respectively. Next, we tested two different uptake mechanisms used by macrophages. First, phagocytosis of fluorescent *E. coli* was not affected by the deletion of IKK2 at two different multiplicities of infection (Figure 5d). Cytochalasin D could inhibit the uptake, indicating actin-

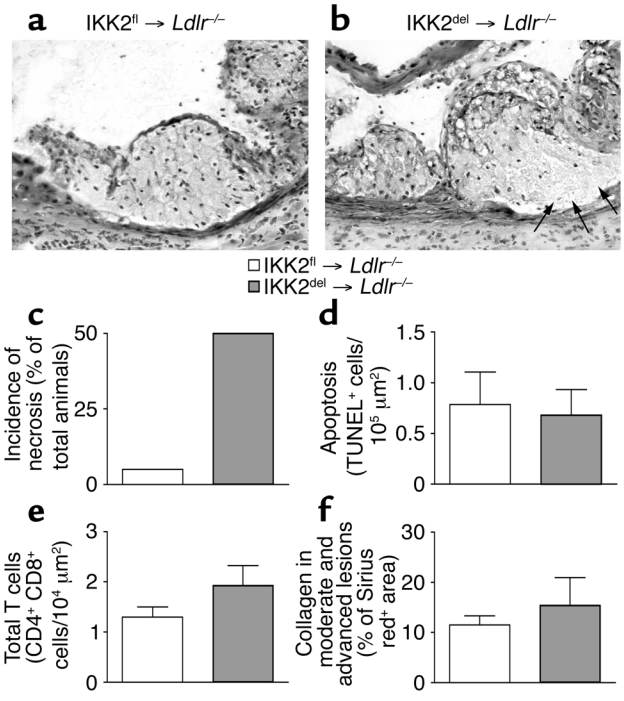

Figure 3
Necrosis, apoptosis, T cells, and collagen in atherosclerotic lesions from IKK2^{fl}- and IKK2^{del}-transplanted *Ldlr*$^{-/-}$ mice. (**a**) Representative lesions from IKK2^{fl}- or (**b**) IKK2^{del}-transplanted mice, showing signs of necrosis (arrows) in the IKK2^{del}-transplanted mice. (**c**) Number of mice for each group that showed signs of necrosis (pyknosis, karyorrhexis, or complete absence of nuclei). (**d**) Apoptosis was detected by TUNEL staining. Bars represent number of TUNEL-positive cells per lesion area. Shown are positive cells in the lesions from IKK2^{fl}- ($n = 15$) and IKK2^{del}- ($n = 11$) transplanted *Ldlr*$^{-/-}$ mice. (**e**) T cells were detected by staining for CD4 and CD8. Shown are cumulative numbers of positive cells in the lesions from IKK2^{fl}- ($n = 20$) and IKK2^{del}- ($n = 18$) transplanted *Ldlr*$^{-/-}$ mice. (**f**) Collagen in the lesions was detected by Sirius red staining and quantified using Scion Image (Scion Corp.). Shown is the Sirius red-positive area as a percentage of the total lesion area in the advanced plaques in lesions from IKK2^{fl}- ($n = 16$) and IKK2^{del}- ($n = 14$) transplanted *Ldlr*$^{-/-}$ mice. Error bars indicate SEM.

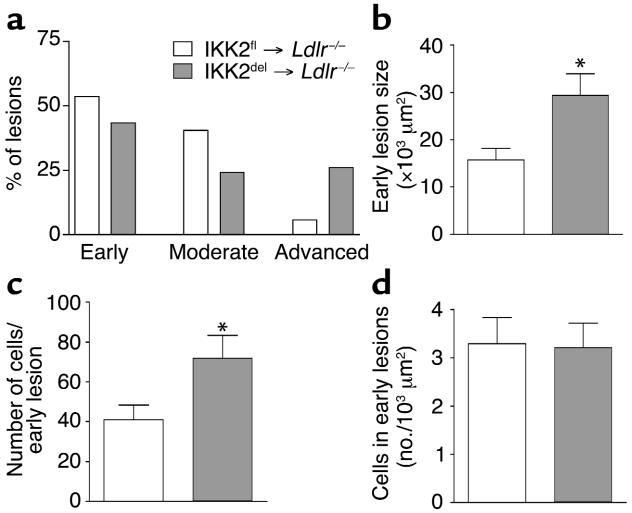

Figure 4
Lesion classification and analysis of early lesions. (**a**) Lesions were typed according to their severity. Shown is the lesion distribution as a percentage of the total number of lesions. (**b**) Size of early lesions in IKK2^{fl}- (n = 16) and IKK2^{del}- (n = 15) transplanted *Ldlr*$^{-/-}$ mice. (**c**) Number of cells in early lesions in IKK2^{fl}- (n = 16) and IKK2^{del}- (n = 15) transplanted *Ldlr*$^{-/-}$ mice. (**d**) Number of cells per lesion area in early lesions. Error bars indicate SEM. *P < 0.05.

dependent phagocytosis and not just binding to the cell surface. Second, we examined endocytosis of modified lipoproteins. At two different doses we could not detect a difference between both IKK2^{fl} and IKK2^{del} macrophages in the uptake of both oxidized LDL (oxLDL) and acetylated LDL (Figure 5e). These data show that IKK2^{del} macrophages are normal in several tested general macrophage functions; they appear to differentiate normally and have normal capacity for phagocytosis of bacteria and receptor-mediated endocytosis of modified LDL.

Deletion of IKK2 in BMM results in susceptibility to LPS-induced cell death after oxLDL loading. To investigate whether deletion of IKK2 would affect cell death in BMM, the cells were subjected to different treatments. Cells were first subjected to oxLDL for 24 hours to induce foam cell formation. After this period, the medium was refreshed, and cells were activated with

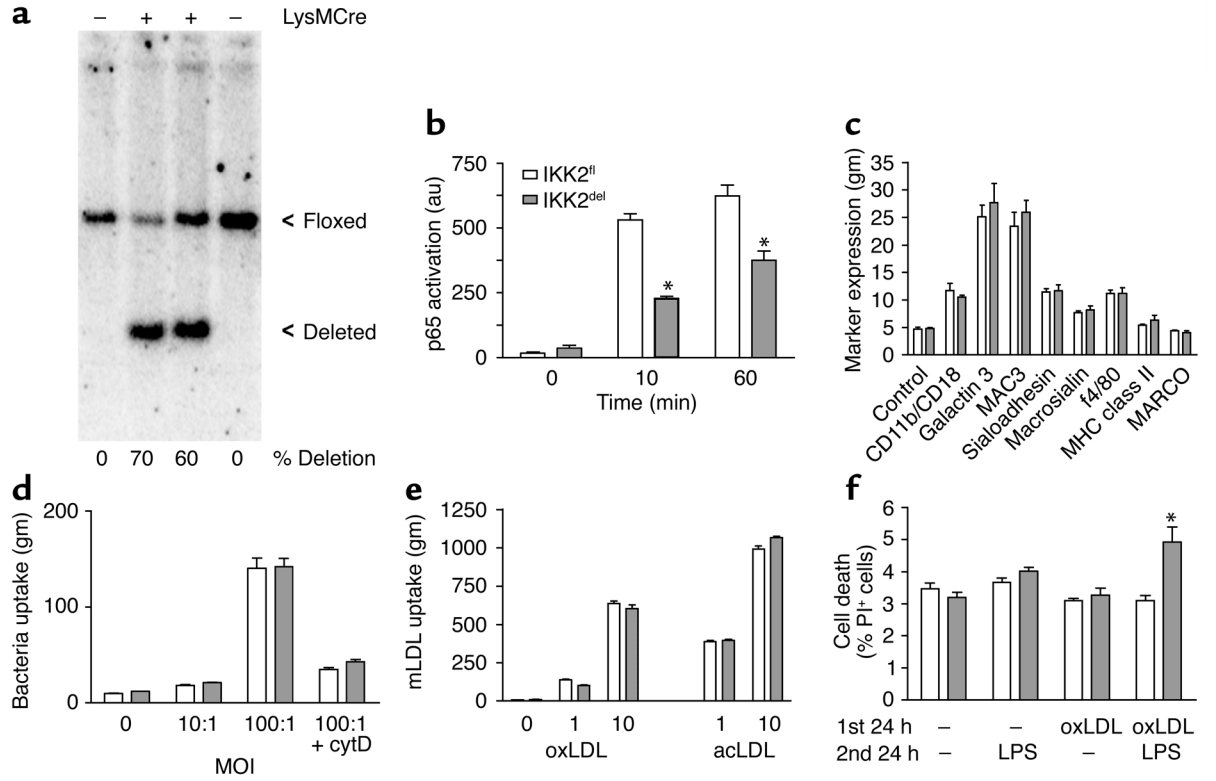

Figure 5
In vitro characterization of IKK2^{fl} and IKK2^{del} macrophages. (**a**) Southern blot of IKK2^{fl} and IKK2^{del} macrophages. Indicated are the presence or absence (+ or –) of Cre-recombinase in the macrophages, the floxed and deleted allele, and the percentage of deletion calculated by quantification of the ratio between the floxed and deleted band. (**b**) Cells were stimulated with LPS for the indicated times, and p65 activation was quantified in nuclear extracts using Trans-am assay. Shown are absorbances after background subtraction. (**c**) Expression of macrophage differentiation markers was quantified by staining for the indicated markers. (**d**) Uptake of different multiplicity of infection of green fluorescent protein expressing *E. coli* by IKK2^{fl} and IKK2^{del} macrophages. (**e**) Uptake of DiI-labeled oxidized LDL (oxLDL) and acetylated LDL (acLDL) by IKK2^{fl} and IKK2^{del} macrophages. (**f**) Cell death of IKK2^{fl} and IKK2^{del} macrophages after indicated incubations with oxLDL (25 μg/ml) and/or LPS (10 ng/ml), determined by propidium iodide (PI) staining. au, arbitrary units; gm, geomean; cytD, cytochalasin D. Error bars indicate SEM. Figures are representative for two experiments. *P < 0.01.

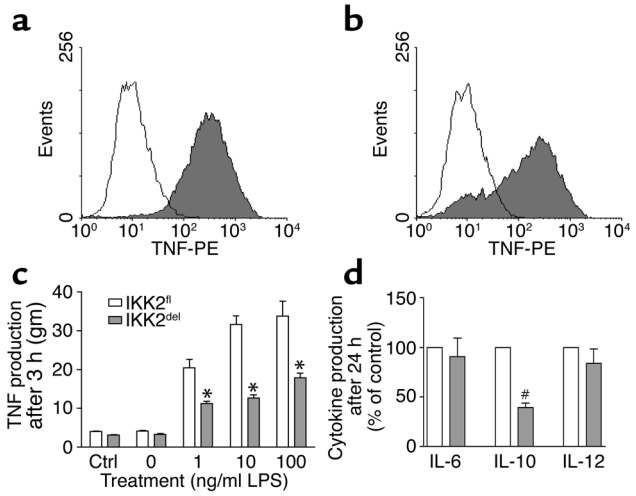

Figure 6
Cytokine production by LPS-stimulated BMM from IKK2^{fl} and IKK2^{del} mice. (**a**) IKK2^{fl} and (**b**) IKK2^{del} macrophages were left untreated (white) or stimulated with LPS (gray). TNF production was detected by intracellular cytokine staining and analyzed by FACS. (**c**) IKK2^{fl} and IKK2^{del} macrophages were stimulated with LPS. TNF production was detected by intracellular cytokine staining and analyzed by FACS. Results are representative for at least two experiments. (**d**) IKK2^{fl} and IKK2^{del} macrophages were stimulated overnight with LPS. Cytokines were measured in the supernatants. Shown are the changes in cytokine production by IKK2^{del} macrophages as compared with IKK2^{fl} macrophages. Results are the average of five to eight experiments. Error bars indicate SEM. $^{*}P < 0.01$; $^{\#}P < 0.01$ by paired *t* test.

LPS or left untreated. Some 24 hours later, we quantified cell death by propidium iodide staining and subsequent FACS analysis (Figure 5f). Interestingly, oxLDL treatment alone or LPS activation alone did not induce major changes or differences in cell death. However, the combination revealed an increased death in IKK2^{del} macrophages. These data indicate that IKK2^{del} foam cells are more prone to activation-induced cell death, which is in good agreement with the in vivo observation of increased necrosis in the lesions of IKK2^{del}-transplanted mice.

Inhibition of NF-κB activation changes the inflammatory phenotype of macrophages. To study the inflammatory capacity of IKK2^{del} macrophages, we activated BMM with LPS and quantified the production of cytokines. TNF is one of the first cytokines secreted upon macrophage activation. We quantified TNF production after 3 hours stimulation with LPS by intracellular cytokine staining (Figure 6a, b, and c). At different doses of LPS, IKK2^{del} macrophages showed a strong (>50%) reduction in total TNF production (Figure 6c). FACS analysis profiles showed that the reduced response in IKK2^{del} macrophages was mainly characterized by the absence of TNF production in approximately 20% of the cells (Figure 6b). These cells are likely completely lacking NF-κB activation due to absence of IKK2. To confirm that these TNF^{-} cells were indeed homozygous deleted for IKK2, TNF^{-} and TNF^{+} cells from IKK2^{del} macrophages were separated and collected by FACS. Quantification of deletion showed that the TNF^{-} cells were approximately 85% deleted, whereas the TNF^{+} were approximately 55% deleted. The incomplete deletion is probably due to the partial overlap of the TNF^{-} and TNF^{+} peaks (Figure 6b). In addition, immunocytochemistry revealed that approximately 20% of IKK2^{del} cells did not show nuclear translocation of p65 after LPS stimulation (not shown), whereas IKK2^{fl} showed >95% translocation.

To see whether the deletion would affect the production of other cytokines, we measured the production of IL-10, IL-6, and IL-12 after LPS stimulation (Figure 6d). We observed a very strong and reproducible reduction in the production of the anti-inflammatory cytokine IL-10. IKK2^{del} macrophages show a 60% decrease in the production of IL-10. There was no significant difference in the production of IL-6 and IL-12 after 24 hours stimulation. Since IL-6 is known to be regulated by NF-κB, we investigated IL-6 production at earlier time points (Figure 7a). Indeed, IL-6 production was reduced in IKK2^{del} macrophages at 3 and 6 hours, respectively after stimulation, but this difference disappears after 24 hours. In view of the fact that IL-10

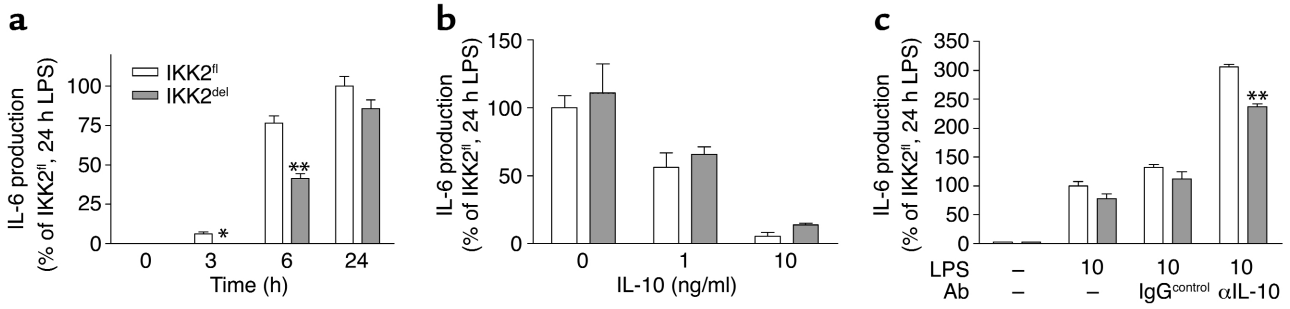

Figure 7
IL-6 production and effects of IL-10. (**a**) IKK2^{fl} and IKK2^{del} macrophages were stimulated with LPS for indicated times. IL-6 was measured in the supernatants. (**b**) IKK2^{fl} and IKK2^{del} macrophages were stimulated with LPS for 24 hours in combination with indicated doses of recombinant mouse IL-10. IL-6 was measured in the supernatants. (**c**) IKK2^{fl} and IKK2^{del} macrophages were stimulated with LPS for 24 hours, in the absence or presence of blocking anti-IL-10 antibody or IgG control. IL-6 was measured in the supernatants. Figures are representative for two experiments. Error bars indicate SEM. $^{*}P < 0.05$, $^{**}P < 0.01$.

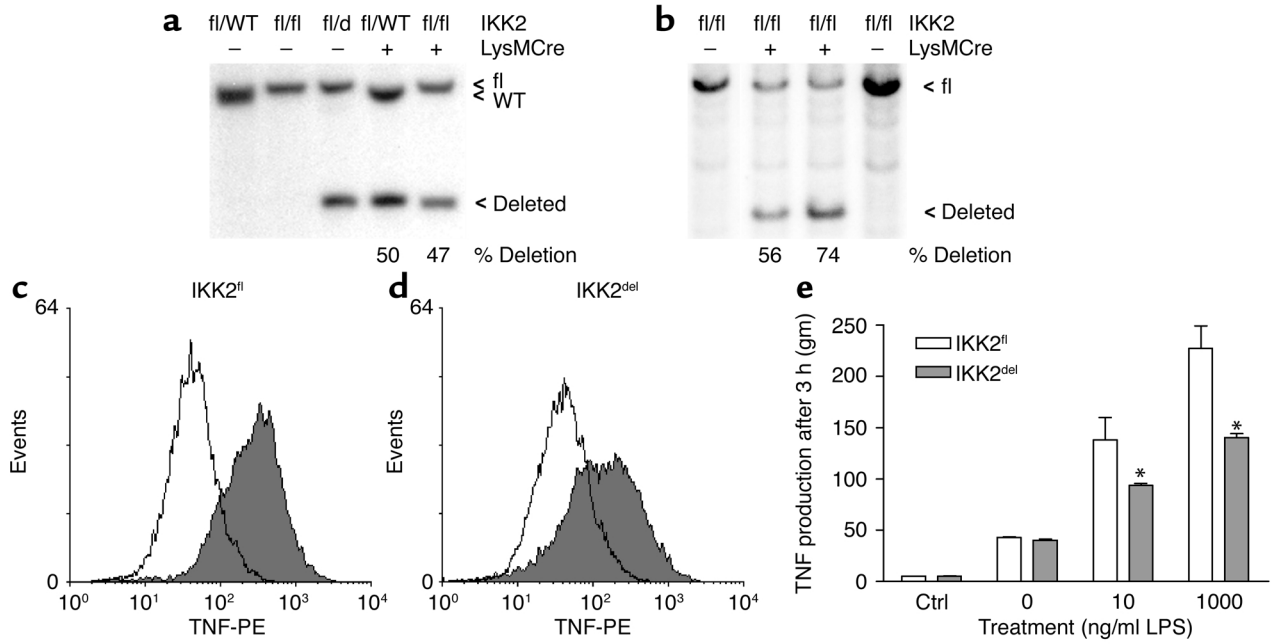

Figure 8

Characterization of resident peritoneal cells and thioglycollate-elicited peritoneal macrophages. (**a**) Southern blot analysis of deletion in FACS-purified resident peritoneal CD11b^{high} cells from mice with the indicated genotypes and (**b**) in thioglycollate-elicited IKK2^{fl} and IKK2^{del} peritoneal macrophages. Indicated are the presence or absence (+ or –) of Cre-recombinase in the macrophages, the WT, floxed (fl), and deleted (d) allele, and the percentage of deletion calculated by quantification of the ratio between the floxed and deleted band. IKK2^{fl} (**c**) and IKK2^{del} (**d**) thioglycollate-elicited macrophages were untreated (white) or stimulated with LPS (gray). TNF production was detected by intracellular cytokine staining and analyzed by FACS. (**e**) IKK2^{fl} and IKK2^{del} macrophages were stimulated with LPS, and TNF production was detected by intracellular cytokine staining and analyzed by FACS. Macrophages were identified as F4/80^{+}. Results are representative for at least two experiments. Error bars indicate SEM. *$P < 0.01$.

was the major cytokine we found to be different after 24 hours, we hypothesized that the absence of difference in IL-6 secretion after 24 hours was due to differential IL-10–mediated autocrine deactivation in IKK2^{fl} and IKK2^{del} macrophages. We found that adding IL-10 exogenously to the macrophages inhibits IL-6 secretion (Figure 7b), confirming deactivation capacity of IL-10. Moreover, inhibition of endogenously secreted IL-10 by blocking antibodies strongly increased IL-6 production and could even restore a difference between IKK2^{fl} and IKK2^{del} macrophages after 24 hours (Figure 7c). These data show that the absence of an effect of IKK2 deletion after 24 hours stimulation is probably due to different autocrine deactivation by IL-10. IKK2^{del} macrophages may initially produce less IL-6 but are also less deactivated due to the strong reduction in IL-10 secretion. In contrast, IKK2^{fl} macrophages may initially produce more IL-6 but are much more deactivated due to increased production of IL-10.

During different assays measuring LPS-induced cytokine production, we could not detect a difference in the amount of cell death between IKK2^{fl} or IKK2^{del} macrophages, as quantified by propidium iodide staining (not shown). In addition, all of the aforementioned changes in cytokine production were caused by deletion of IKK2 and not by expression of Cre-recombinase in the IKK2^{del} macrophages since, in the cytokine production assays, WT macrophages expressing Cre-recombinase were not different from WT cells not expressing Cre (not shown).

Deletion and activation of in vivo differentiated macrophages. Deletion in in vivo differentiated cells was quantified by sorting of CD11b^{high}/CD19^{-} resident peritoneal cells from different mice and subsequent Southern blotting (Figure 8a). Deletion of the floxed allele in cells from heterozygous IKK2 mice (IKK2$^{fl/WT}$) expressing Cre-recombinase was complete (Figure 8a). However, macrophages from homozygously floxed IKK2 mice (IKK2$^{fl/fl}$) (Figure 8a), and macrophages from mice with one floxed and one germ line deleted allele (IKK2$^{fl/-}$/LysMCre), showed only partial deletion of the loxP-flanked IKK2 alleles (data not shown) suggesting that cells lacking IKK2 are counterselected. Experiments performed in mice carrying a second IKK2 conditional allele, IKK2ΔKfl (24), which upon deletion produces a kinase-dead mutant IKK2, showed similar results (data not shown), further supporting that macrophages with compromised IKK signaling are counterselected in vivo. To investigate whether in vivo differentiated inflammatory macrophages are impaired in their LPS response, we isolated thioglycollate-elicited peritoneal cells from IKK2^{fl} and IKK2^{del} mice. Adherent cells from peritoneal lavages showed similar deletion percentages as BMM

(Figure 8b) and contained >95% macrophages ($F4/80^+$). Cells were cultured for 20 hours and activated with LPS. After 3 hours, TNF production was quantified in $F4/80^+$ cells (Figure 8c, d, and e). Again, a reduction was observed, confirming that in vivo differentiated $IKK2^{del}$ macrophages are also impaired in their inflammatory response.

Discussion

In this article, we addressed the role of IKK2-mediated NF-κB activation in macrophages in the pathogenesis of atherosclerosis by using macrophage-specific deletion of IKK2. We found that inhibition of NF-κB in macrophages causes more severe atherosclerosis, which is characterized by increased lesion size, more severe lesions, increased necrosis, and more macrophages in the early lesions.

Our data represent the first mouse model investigating the role of macrophage NF-κB activation in atherosclerosis. Several lines of circumstantial evidence have indicated a potential role for NF-κB in atherosclerosis. First of all, activated NF-κB has been demonstrated in human atherosclerotic plaques, in macrophages, smooth muscle cells, and endothelial cells (5). Moreover, several NF-κB regulated genes have been demonstrated to be upregulated in plaques, including proinflammatory cytokines, such as TNF and IL-6 (25). Additionally, receptors that can signal to NF-κB are also present in lesions, including several member of the toll-like receptor family, which also mediate LPS-induced activation of macrophages (26). However, how this network of activating agents, receptors, and NF-κB signaling actually controls atherogenesis remains unclear. For example, both TNF and IL-6 are present in plaques and considered proinflammatory cytokines. Yet animals deficient for these cytokines are not affected in their atherosclerosis when early lesions are analyzed (27, 28). In contrast, IL-6 deficient mice even develop more atherosclerosis when later stages of atherosclerosis are examined and mice deficient for one of the TNF receptors, TNFR55, also develop more atherosclerosis (29). The role of the anti-inflammatory cytokine IL-10 may be more straightforward. Previous reports have shown that absence of IL-10 strongly aggravates atherosclerosis (30). Therefore, our observed effects of IKK2 deletion in macrophages resulting in a reduction in IL-10 can be regarded as pro-atherogenic and may explain our observed increase in atherosclerosis. However, through which mechanisms and genes NF-κB is involved in the regulation of atherogenesis remains a challenging question for future research.

$IKK2^{del}$ macrophages exhibit a strong (>50%) reduction in TNF production, showing that although the deletion is only 65%, activation of NF-κB responsive genes is highly affected. Why the deletion was not complete is not clear, but it is similar to the deletion efficiency in BMM as previously reported using the same LysMCre strain (10). In these experiments deletion was nearly complete in in vivo differentiated cells, that is, resident peritoneal macrophages. In agreement with these results, we found that deletion of the floxed allele in $CD11b^{high}$-resident peritoneal cells from heterozygous floxed mice ($IKK2^{fl/WT}$/LysMCre) is nearly complete (Figure 6a). However, we found that deletion in $IKK2^{fl/fl}$/LysMCre mice is only 50% in resident cells and up to 70% in inflammatory cells. In addition, we observed that deletion in cells from mice carrying one deleted and one floxed allele in their germ line ($IKK2^{fl/del}$/LysMCre) is approximately 70% (M. Pasparakis, unpublished observation). Finally, we observed, in vivo in atherosclerotic lesions and in vitro in activated foam cells, increased necrosis upon deletion of IKK2. These data support the possibility of selection against homozygous deleted IKK2-deficient macrophages. Under which exact circumstances this is happening and how it is triggered remains to be elucidated.

The observation that long-term (i.e., 24-hour) production of proinflammatory cytokines IL-6 and IL-12 is not affected may very well be a reflection of a reduced autocrine deactivation of $IKK2^{del}$ macrophages caused by the reduced IL-10 production. Several reports have now shown that IL-10 can deactivate macrophages in an autocrine fashion, reducing secretion of several proinflammatory cytokines, including IL-6 and IL-12 (31, 32). Indeed, we could also confirm these mechanisms (Figure 7). Initial IL-6 production is reduced as expected (i.e., similarly as the decrease in NF-κB activation, Figure 5b), but at 24 hours, when IL-10 has exerted its autocrine effect, the difference is gone. Also, exogenously added IL-10 could completely block IL-6 production, indicating the inhibitory potential of IL-10. Most interestingly, blockage of endogenously produced IL-10 by antibodies strongly increased IL-6 production and even restored a difference between $IKK2^{fl}$ and $IKK2^{del}$ macrophages after 24 hours stimulation. In conclusion, the net end result of the deletion of IKK2 in our macrophage population is a major reduction in the secretion of the anti-inflammatory cytokine IL-10 and not in the secretion of the proinflammatory cytokines IL-6 and IL-12. How this may be affected by incomplete deletion of IKK2 or by other autocrine regulatory mechanisms is still unclear.

In line with our in vitro data regarding the decrease in IL-10, inhibition of macrophage NF-κB activation resulted in an increase in atherosclerosis. The lesions in $IKK2^{del}$-transplanted mice were more severe but also showed increased cell numbers in the early lesions. The latter may indicate an enhanced influx of monocytes in the early phases of lesion formation or enhanced proliferation. An additional factor exacerbating atherosclerosis in the $IKK2^{del}$ mice may be the observed increase in necrosis. Necrotic areas in the plaque can act in a proinflammatory manner and enhance progression of lesion formation. Differences in intracellular lipid accumulation will probably not be the cause of necrosis in the $IKK2^{del}$ mice, since we do not see differences in the uptake of modified LDL (Figure 5e) and lipid loading after 24 or 48 hours incubation with

oxidized or acetylated LDL was also not different between groups (E. Kanters and M.P.J. de Winther, unpublished data). The mechanism of increased necrosis in the plaque remains unclear but was confirmed in vitro using LPS-activated foam cells, which showed increased cell death in the absence of IKK2.

Recently, the role of NF-κB in controlling inflammation has been described. Lawrence et al. (33) used a carrageenin-induced inflammatory model. They showed that during inflammation, early NF-κB activation is associated with an increased influx of inflammatory cells and activation of several proinflammatory genes. In contrast, NF-κB activation later during the process was associated with the resolution of inflammation and expression of anti-inflammatory genes. These data show that NF-κB acts as an anti-inflammatory regulator of the resolution of inflammation.

In conclusion, we demonstrate that inhibition of IKK2-mediated NF-κB activation in macrophages enhances atherosclerosis. The described mouse model will be a valuable tool to investigate the exact mechanisms that control inflammation and cell death during the process of atherosclerotic plaque formation.

Acknowledgments

This work was supported by the Dutch Organization for Scientific Research (NWO 902-26-194) and the European Union (MAFAPS-QLG1-99-001007). M. Pasparakis received fellowship awards from the European Molecular Biology Organization and from the Leukemia and Lymphoma Society. R.J.A. Fijneman is supported by the Dutch Cancer Society (VU2000-2350). M.H. Hofker is an Established Investigator of the Dutch Heart Association (NHS D95022). M.P.J. de Winther is an NWO fellow (906-02-075). The authors thank Cornelis van 't Veer for help and advice on autocrine deactivation and blocking IL-10 antibodies and Heinz Jacobs for critically reading the manuscript and fruitful discussion. Ingeborg van der Made and Patrick van Gorp are thanked for technical assistance.

1. Lusis, A.J. 2000. Atherosclerosis. *Nature.* **407**:233–241.
2. Ross, R. 1993. The pathogenesis of atherosclerosis: a perspective for the 1990s. *Nature.* **362**:801–809.
3. Libby, P. 2002. Inflammation in atherosclerosis. *Nature.* **420**:868–874.
4. Collins, T., and Cybulsky, M.I. 2001. NF-kappaB: pivotal mediator or innocent bystander in atherogenesis? *J. Clin. Invest.* **107**:255–264.
5. Brand, K., et al. 1996. Activated transcription factor nuclear factor-kappa B is present in the atherosclerotic lesion. *J. Clin. Invest.* **97**:1715–1722.
6. Karin, M., and Ben-Neriah, Y. 2000. Phosphorylation meets ubiquitination: the control of NF-[kappa]B activity. *Annu. Rev. Immunol.* **18**:621–663.
7. Li, Q., Van Antwerp, D., Mercurio, F., Lee, K.F., and Verma, I.M. 1999. Severe liver degeneration in mice lacking the IkappaB kinase 2 gene. *Science.* **284**:321–325.
8. Li, Z.W., et al. 1999. The IKKbeta subunit of IkappaB kinase (IKK) is essential for nuclear factor kappaB activation and prevention of apoptosis. *J. Exp. Med.* **189**:1839–1845.
9. Pasparakis, M., et al. 2002. TNF-mediated inflammatory skin disease in mice with epidermis-specific deletion of IKK2. *Nature.* **417**:861–866.
10. Clausen, B.E., Burkhardt, C., Reith, W., Renkawitz, R., and Forster, I. 1999. Conditional gene targeting in macrophages and granulocytes using LysMcre mice. *Transgenic Res.* **8**:265–277.
11. Ishibashi, S., et al. 1993. Hypercholesterolemia in low density lipoprotein receptor knockout mice and its reversal by adenovirus-mediated gene delivery. *J. Clin. Invest.* **92**:883–893.
12. de Winther, M.P., et al. 1999. Scavenger receptor deficiency leads to more complex atherosclerotic lesions in APOE3Leiden transgenic mice. *Atherosclerosis.* **144**:315–321.
13. Gijbels, M.J., et al. 1999. Progression and regression of atherosclerosis in APOE3-Leiden transgenic mice: an immunohistochemical study. *Atherosclerosis.* **143**:15–25.
14. Kockx, M.M., Muhring, J., Knaapen, M.W., and de Meyer, G.R. 1998. RNA synthesis and splicing interferes with DNA in situ end labeling techniques used to detect apoptosis. *Am. J. Pathol.* **152**:885–888.
15. Peiser, L., Gough, P.J., Kodama, T., and Gordon, S. 2000. Macrophage class A scavenger receptor-mediated phagocytosis of Escherichia coli: role of cell heterogeneity, microbial strain, and culture conditions in vitro. *Infect. Immun.* **68**:1953–1963.
16. Hume, D.A., and Gordon, S. 1983. Optimal conditions for proliferation of bone marrow-derived mouse macrophages in culture: the roles of CSF-1, serum, Ca2+, and adherence. *J. Cell Physiol.* **117**:189–194.
17. Schmidt-Supprian, M., et al. 2000. NEMO/IKK gamma-deficient mice model incontinentia pigmenti. *Mol. Cell.* **5**:981–992.
18. Hendriks, W.L., van der Boom, H., van Vark, L.C., and Havekes, L.M. 1996. Lipoprotein lipase stimulates the binding and uptake of moderately oxidized low-density lipoprotein by J774 macrophages. *Biochem. J.* **314**:563–568.
19. Steinbrecher, U.P., Witztum, J.L., Parthasarathy, S., and Steinberg, D. 1987. Decrease in reactive amino groups during oxidation or endothelial cell modification of LDL. Correlation with changes in receptor-mediated catabolism. *Arteriosclerosis.* **7**:135–143.
20. Underhill, D.M., et al. 1999. The toll-like receptor 2 is recruited to macrophage phagosomes and discriminates between pathogens. *Nature.* **401**:811–815.
21. Beg, A.A., Sha, W.C., Bronson, R.T., Ghosh, S., and Baltimore, D. 1995. Embryonic lethality and liver degeneration in mice lacking the RelA component of NF-kappa B. *Nature.* **376**:167–170.
22. Tanaka, M., et al. 1999. Embryonic lethality, liver degeneration, and impaired NF-kappa B activation in IKK-beta-deficient mice. *Immunity.* **10**:421–429.
23. van Vlijmen, B.J., et al. 1994. Diet-induced hyperlipoproteinemia and atherosclerosis in apolipoprotein E3-Leiden transgenic mice. *J. Clin. Invest.* **93**:1403–1410.
24. Pasparakis, M., Schmidt-Supprian, M., and Rajewsky, K. 2002. IkappaB kinase signaling is essential for maintenance of mature B cells. *J. Exp. Med.* **196**:743–752.
25. Zhou, X., and Hansson, G.K. 1999. Detection of B cells and proinflammatory cytokines in atherosclerotic plaques of hypercholesterolaemic apolipoprotein E knockout mice. *Scand. J. Immunol.* **50**:25–30.
26. Edfeldt, K., Swedenborg, J., Hansson, G.K., and Yan, Z.Q. 2002. Expression of toll-like receptors in human atherosclerotic lesions: a possible pathway for plaque activation. *Circulation.* **105**:1158–1161.
27. Elhage, R., et al. 2001. Involvement of interleukin-6 in atherosclerosis but not in the prevention of fatty streak formation by 17beta-estradiol in apolipoprotein E-deficient mice. *Atherosclerosis.* **156**:315–320.
28. Schreyer, S.A., Vick, C.M., and LeBoeuf, R.C. 2002. Loss of lymphotoxin-alpha but not tumor necrosis factor-alpha reduces atherosclerosis in mice. *J. Biol. Chem.* **277**:12364–12368.
29. Schreyer, S.A., Peschon, J.J., and LeBoeuf, R.C. 1996. Accelerated atherosclerosis in mice lacking tumor necrosis factor receptor p55. *J. Biol. Chem.* **271**:26174–26178.
30. Mallat, Z., et al. 1999. Protective role of interleukin-10 in atherosclerosis. *Circ. Res.* **85**:e17–e24.
31. Lang, R., Rutschman, R.L., Greaves, D.R., and Murray, P.J. 2002. Autocrine deactivation of macrophages in transgenic mice constitutively overexpressing IL-10 under control of the human CD68 promoter. *J. Immunol.* **168**:3402–3411.
32. Giambartolomei, G.H., Dennis, V.A., Lasater, B.L., Murthy, P.K., and Philipp, M.T. 2002. Autocrine and exocrine regulation of interleukin-10 production in THP-1 cells stimulated with Borrelia burgdorferi lipoproteins. *Infect. Immun.* **70**:1881–1888.
33. Lawrence, T., Gilroy, D.W., Colville-Nash, P.R., and Willoughby, D.A. 2001. Possible new role for NF-kappaB in the resolution of inflammation. *Nat. Med.* **7**:1291–1297.